Neurosci. Bull. February, 2016, 32(1):83–91
DOI 10.1007/s12264-016-0013-1

www.neurosci.cn
www.springer.com/12264

ORIGINAL ARTICLE

Rho-Associated Kinase Inhibitors Promote Microglial Uptake *Via* the ERK Signaling Pathway

Peicai Fu[1] · Ronghua Tang[1] · Zhiyuan Yu[1,2] · Caihong Li[1] · Xue Chen[1] · Minjie Xie[1,2] · Wei Wang[1,2] · Xiang Luo[1]

Received: 3 June 2015 / Accepted: 26 November 2015 / Published online: 18 January 2016

Abstract Microglia are immunocompetent cells in the central nervous system that take up tissue debris and pathogens. Rho-associated kinase (ROCK) has been identified as an important regulator of uptake, proliferation, secretion, and differentiation in a number of cell types. Although ROCK plays critical roles in the microglial secretion of inflammatory factors, migration, and morphology, its effects on microglial uptake activity have not been well characterized. In the present study, we found that treatment of BV2 microglia and primary microglia with the ROCK inhibitors Y27632 and fasudil increased uptake activity and was associated with morphological changes. Furthermore, western blots showed that this increase in uptake activity was mediated through the extracellular-signal-regulated kinase (ERK) signaling cascade, indicating the importance of ROCK in regulating microglial uptake activity.

Keywords Microglia · Rho-associated kinase · Uptake activity · Extracellular-signal-regulated kinase

Introduction

Microglia are immunocompetent cells in the central nervous system (CNS) and have many functional properties in common with peripheral macrophages [1, 2]. A major innate immune function of microglia is the receptor-mediated uptake of tissue debris and pathogens in the CNS [3]. Rapid and efficient uptake protects against neuronal damage, and contributes to tissue remodeling and immune response regulation [4]. Uptake, like other modes of cytokinesis, depends on mechanical forces generated by stress fibers [5–7]. Stress fibers are dynamic structures whose assembly/disassembly and functions are regulated by the small GTPase RhoA and its major effector Rho-kinase (ROCK).

Rho-associated coiled-coil forming protein serine/threonine kinase (ROCK, rho-associated kinase), a well-characterized downstream effector of Rho, is a mixture of two highly homologous isoforms: ROCK1 and ROCK2 [8, 9]. The activation of ROCK is known to phosphorylate the regulatory myosin light chain (MLC) and the myosin-binding subunit of the MLC phosphatase to inhibit its catalytic activity. Therefore, ROCK contributes to a number of actin–myosin-mediated processes, such as cell motility, adhesion, proliferation, differentiation, neurite retraction, and uptake [10]. The uptake activity is regulated by the cytoskeleton through MLC kinase. Accumulating evidence indicates that ROCK plays a central role during uptake in different cell types [11–16]. However, its role in microglial uptake and its possible mechanism are not fully understood.

In this study, we investigated the effects of ROCK inhibition on the uptake activity of BV2 cells (a microglial cell line) and primary microglia using Y27632 (a specific ROCK inhibitor) and fasudil (a nonspecific ROCK inhibitor), which are widely used to study the functions of ROCK signaling [17, 18].

Materials and Methods

Culture of BV2 Microglia

The microglial cell line BV2 was purchased from the Chinese Academy of Medical Sciences, Beijing, China.

✉ Xiang Luo
tjhfile@tjh.tjmu.edu.cn

[1] Department of Neurology, Tongji Hospital, Tongji Medical College, Huazhong University of Science and Technology, Wuhan 430030, China

[2] Key Laboratory of Neurological Diseases (HUST), Ministry of Education of China, Wuhan 430030, China

After recovery from liquid nitrogen, cells were cultured in high-glucose Dulbecco's modified Eagle's medium (DMEM) supplemented with 10% fetal bovine serum (FBS) at 37 °C in a 95% O_2 and 5% CO_2 atmosphere. The medium was changed every 2 days until confluence. The cells were found to be Iba1-positive (ionized calcium binding adaptor molecule, 1:300; Wako, Richmond, VA) microglia. ROCK2 expression was assessed by immunostaining with rabbit anti-ROCK2 antibody (1:300; Santa Cruz Biotechnology, Santa Cruz, CA).

Lactate dehydrogenase (LDH) release was measured using a CytoTox 96 nonradioactive cytotoxicity assay kit (Promega, Madison, WI) to assess the toxicity caused by 10 μmol/L Y27632 (Sigma Chemical, St. Louis, MO) [19, 20] and 41 μmol/L fasudil (Sigma Chemical) [21]. The ROCK Activity Assay kit (Millipore, Chemicon, Billerica, MA) was used to assess ROCK activity changes induced by Y27632 and fasudil as indicated by the manufacturer.

Culture of Primary Microglia

The brains of newborn Sprague-Dawley pups were dissociated, and cells were cultured in mixture. After two days, the medium was refreshed with high-glucose DMEM containing 20% FBS. Ten days later without medium change, microglial cells were isolated by an orbital shaker (37 °C, 200 rpm, 1.5 h). Twenty minutes after cells attached on the dishes, the medium was refreshed with high-glucose DMEM containing 10% FBS for further purification. After identification with anti-Iba1 and DAPI, cultures of >95% purity were used for experiments. ROCK2 expression was assessed by immunostaining with rabbit anti-ROCK2 antibody.

FITC–Dextran Uptake Analysis by Flow Cytometry

Uptake was evaluated using FITC–dextran uptake analysis. Briefly, BV2 cells and primary microglial cells were suspended in culture medium, adjusted to a concentration of 1×10^6–5×10^6 cells/mL, plated (2 mL/well) in 6-well cell culture plates, and incubated for 24 h. The cells were randomly assigned to four groups: negative control group, control group, Y27632 (10 μmol/L) group, and fasudil (41 μmol/L) group. The cells in the control, Y27632, and fasudil groups were incubated for 1 h at 37 °C with FITC–dextran (0.1 mg/mL, molecular weight, 40,000, FD-40s; Sigma) [22, 23]. The negative control group was incubated with FITC–dextran at 4 °C for 1 h to exclude extracellular binding of FITC-dextran, and was used to set the baseline value in flow cytometry. Then the cells were extensively washed 3 times with ice-cold PBS. The uptake of FITC–dextran was analyzed using a fluorescence-activated cell analyzer (Becton Dickinson, Franklin Lakes, NJ) and data analysis was performed with Modifit LT 2.0 (Becton Dickinson). For statistical analysis, the level of uptake was determined as FITC–dextran positive cell number/total cell number.

Western Blot

The BV2 cells were used for western blot analysis. To assess the expression of mitogen-activated protein kinase (MAPK)-related proteins, total proteins were extracted using RIPA buffer (50 mmol/L Tris, pH 7.4, 150 mmol/L NaCl, 1% Triton X-100, 1% sodium deoxycholate, and 0.1% SDS) containing 1 mmol/L phenylmethylsulfonyl fluoride. Protein concentrations in the supernatants were determined using the bicinchoninic acid protein assay kit (Pierce, Cheshire, UK) with bovine serum albumin as the standard.

Equal amounts of proteins were separated by 15% SDS-PAGE and transferred to nitrocellulose membranes (Hybond C-Super, Amersham Pharmacia Biotech, Amersham, UK). The membranes were blocked in 5% (*w/v*) nonfat milk in TBST (10 mmol/L Tris-HCl, 150 mmol/L NaCl, and 0.02% [*v/v*] Tween-20, pH 7.5) and incubated overnight at 4 °C with the primary antibodies anti-p-p38 and anti-p38 (1:500, Cell Signaling Technology, Inc., Danvers, MA), anti-p-JNK and anti-JNK (1:500, Cell Signaling Technology, Inc.), anti-p-ERK (1:300, Cell Signaling Technology, Inc.), anti-ERK1/2 (1:500, Santa Cruz Technology), and anti-β-actin (1:1,500, Santa Cruz Technology). Secondary antibodies (IRDye 800-conjugated goat anti-rabbit IgG and/or Alexa Fluor 800-conjugated goat anti-mouse IgG, dilution 1:5,000; Rockland Immunochemicals, Gilbertsville, PA) were added according to the manufacturer's instructions. The immunoreactivity of protein bands was quantified using an Odyssey IR imaging system (LI-COR Biosciences Inc., Lincoln, NE) and expressed as the mean optical density (OD). For statistical analysis, the OD value of each protein was normalized to that of β-actin.

Immunocytochemical Staining

Cells seeded on glass coverslips were incubated in high-glucose DMEM containing 10% FBS and 10 μmol/L Y27632 or 41 μmol/L fasudil for 1 h, with or without pre-incubation with 10 μmol/L U0126 (Promega, Madison, WI), fixed in 100% methanol for 15 min, washed in PBS, incubated with 5% bovine serum albumin in PBS at room temperature for 2 h to block nonspecific antibody binding, incubated overnight with anti-Iba1 or anti-ROCK2 at 4 °C, and then incubated with CY3-conjugated goat anti-rabbit IgG antibody (1:200; Jackson ImmunoResearch Laboratories Inc., West Grove, PA) and DAPI (10 μg/mL; Jackson ImmunoResearch Laboratories Inc.) for 10 min.

Statistical Analysis

All data are expressed as mean ± SEM. Student's paired *t* test was used to compare differences between two groups and one-way ANOVA with Tukey's *post hoc* test was used to compare differences among more than two groups. $P < 0.05$ was considered statistically significant.

Results

Morphological Changes and Increased Uptake by BV2 Microglia after Y27632 and Fasudil Treatment

Immunocytochemical staining indicated that the confluent cells were Iba1-positive (Fig. 1A1) and ROCK2-positive (Fig. 1A2) microglia. The LDH release assay showed no significant difference between the Y27632, fasudil, and control groups (Fig. 1B). Hence, 10 μmol/L Y27632 and 41 μmol/L fasudil were not cytotoxic. To confirm direct inhibition of ROCK by Y27632 and fasudil, we further used the Rho-kinase activity assay kit to detect ROCK activity in BV2 microglial cells. After 0.5, 1, and 3 h of Y27632 and fasudil treatment, the activity of ROCK in BV2 microglia was reduced significantly (Fig. 1C).

Immunocytochemical staining with Iba1/DAPI showed that the Y27632- and fasudil-treated BV2 cells were larger and more irregularly shaped than control cells and had many small dendrites (Fig. 2A1–A3). The flow cytometric analysis of control, Y27632-, and fasudil-treated BV2 cells at 1 h indicated that Y27632 and fasudil stimulated the uptake activity of BV2 cells (Fig. 2B). The Y27632-treated cells had a higher uptake (95.7 ± 1.3% *vs* 61.0 ± 1.8%, $P < 0.01$; Fig. 2C1) and mean fluorescence intensity (26.7 ± 0.3% *vs* 13.3 ± 0.3%, $P < 0.01$; Fig. 2C2) than control cells. Similarly, fasudil-treated cells had higher uptake (96.8 ± 1.3% *vs* 61.0 ± 1.8%, $P < 0.01$; Fig. 2C1) and mean fluorescence intensity (27.7 ± 0.3% *vs* 13.3 ± 0.3%, $P < 0.01$; Fig. 2C2) than controls. These findings demonstrated that ROCK inhibition increases the uptake activity of BV2 cells.

Morphological Changes and Increased Uptake Activity of Primary Microglia after Y27632 and Fasudil Treatment

Although BV2 cells are reported to share many characteristics with primary microglia and represent a suitable model for *in vitro* studies of activated microglial cells, they still exhibit behavior, motility, and gene expression profiles different from primary microglial cells. So we also

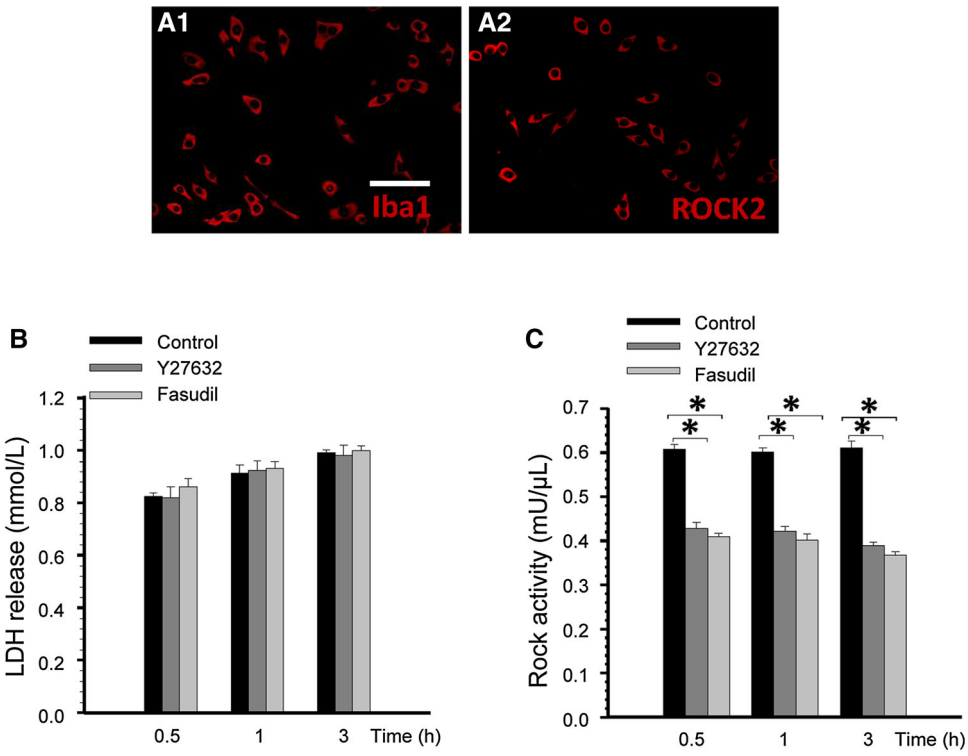

Fig. 1 ROCK2 was expressed in BV2 microglial cells and the ROCK inhibitors were not cytotoxic to BV2 cells. (**A**) Expression of Iba1 and ROCK2 identified by staining with anti-Iba1 (*red*) (**A1**) and anti-ROCK2 (*red*) (**A2**). *Scale bar*, 25 μm. (**B**) Mean LDH release after 0.5, 1, and 3 h of treatment with Y27632 and fasudil ($n = 4$). (**C**) Statistical analysis of ROCK activity in BV2 microglial cells after Y27632 and fasudil treatment. Compared with the control group, ROCK activity was significantly decreased in the Y27632 and fasudil groups ($n = 4$, $^*P < 0.01$).

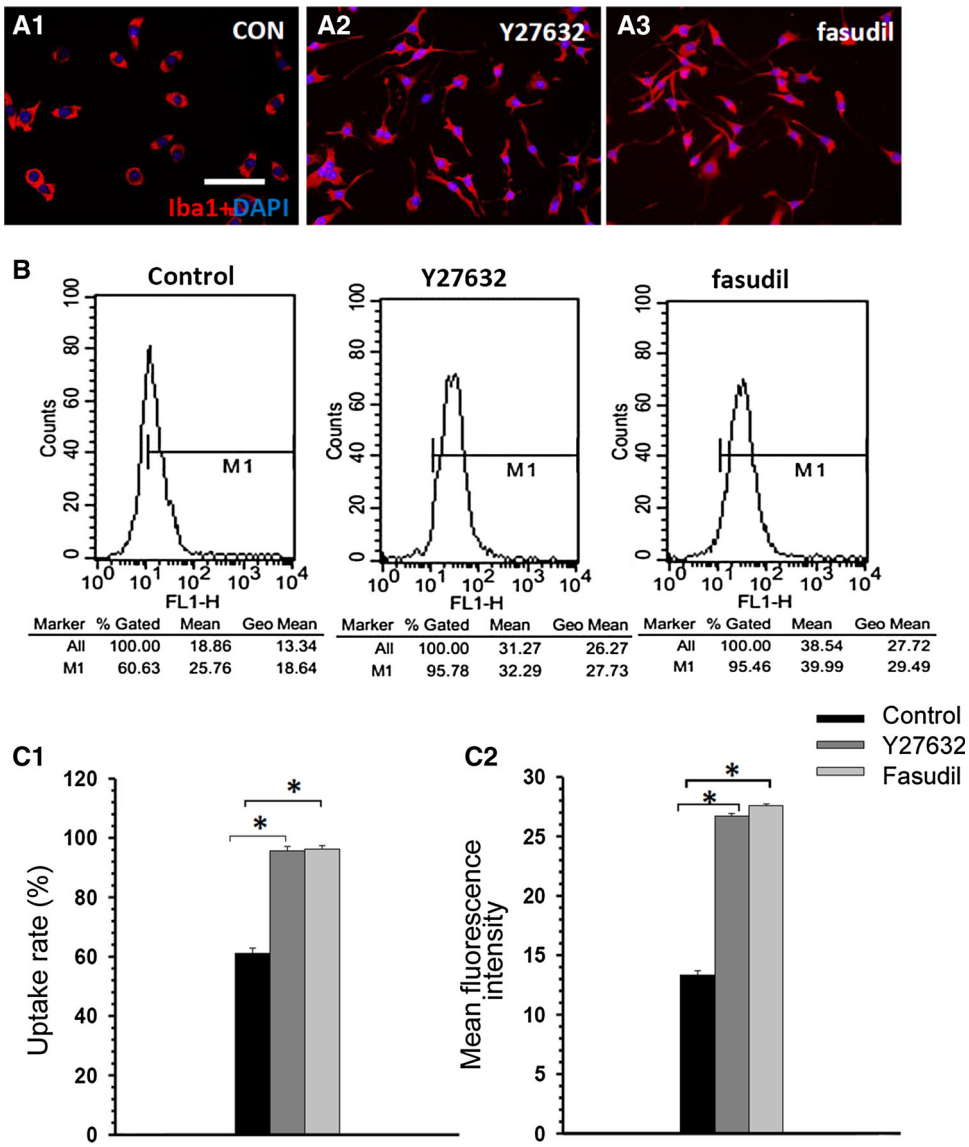

Fig. 2 Y27632 and fasudil changed cell morphology and enhanced uptake activity in BV2 microglia. (**A**) Double staining with Iba1 (*red*) and DAPI (*blue*) 1 h after treatment in the control (**A1**), Y27632 (**A2**), and fasudil (**A3**) groups (*scale bar*, 25 μm). (**B**) Representative examples of flow cytometric analysis of control-, Y27632-, and fasudil-treated BV2 cells at 1 h. (**C**) The data indicated that Y27632 and fasudil stimulated uptake activity in BV2 cells. The percentage of BV2 cells that took up FITC-dextran (**C1**) and the mean fluorescence intensity of FITC-dextran (**C2**) in BV2 cells increased after Y2762 and fasudil treatment. The results are expressed as the mean ± SEM ($n = 5$, $^*P < 0.01$, Y27632 *vs* control group, fasudil *vs* control group).

investigated the effects of Y27632 and fasudil on morphological changes and uptake activity of primary microglia. Immunocytochemical analysis indicated that almost 95% of the confluent cells were ROCK2-positive (Fig. 3A1) and Iba1-positive (Fig. 3B1) primary microglia. Similar to BV2 cells, the Y27632- and fasudil-treated primary microglia were larger and more irregularly shaped than control cells and had many small dendrites (Fig. 3B1–B3). Representative examples of flow cytometric analysis of control, Y27632-, and fasudil-treated primary microglia at 1 h are shown in Fig. 3C. The Y27632-treated microglia had a higher uptake (87.9 ± 1.1% *vs* 50.3 ± 1.7%, $P < 0.01$; Fig. 3D1) and mean fluorescence intensity (24.1 ± 1.1% *vs* 10.6 ± 0.7%, $P < 0.01$; Fig. 3D2) than control cells. Similarly, fasudil-treated microglia had a higher uptake rate (88.3 ± 1.3% *vs* 50.3 ± 1.7%, $P < 0.01$; Fig. 3D1) and mean fluorescence intensity (26.2 ± 0.8% *vs* 10.6 ± 0.7%, $P < 0.01$; Fig. 3D2) than control cells. These findings demonstrated that ROCK inhibition changes cell morphology and increases the uptake activity of primary microglia.

Involvement of the ERK Signaling Pathway in Y27632- and Fasudil-Induced Uptake Enhancement

MAPK-related cell-signal proteins have been implicated in microglial proliferation, inflammatory factor secretion, and

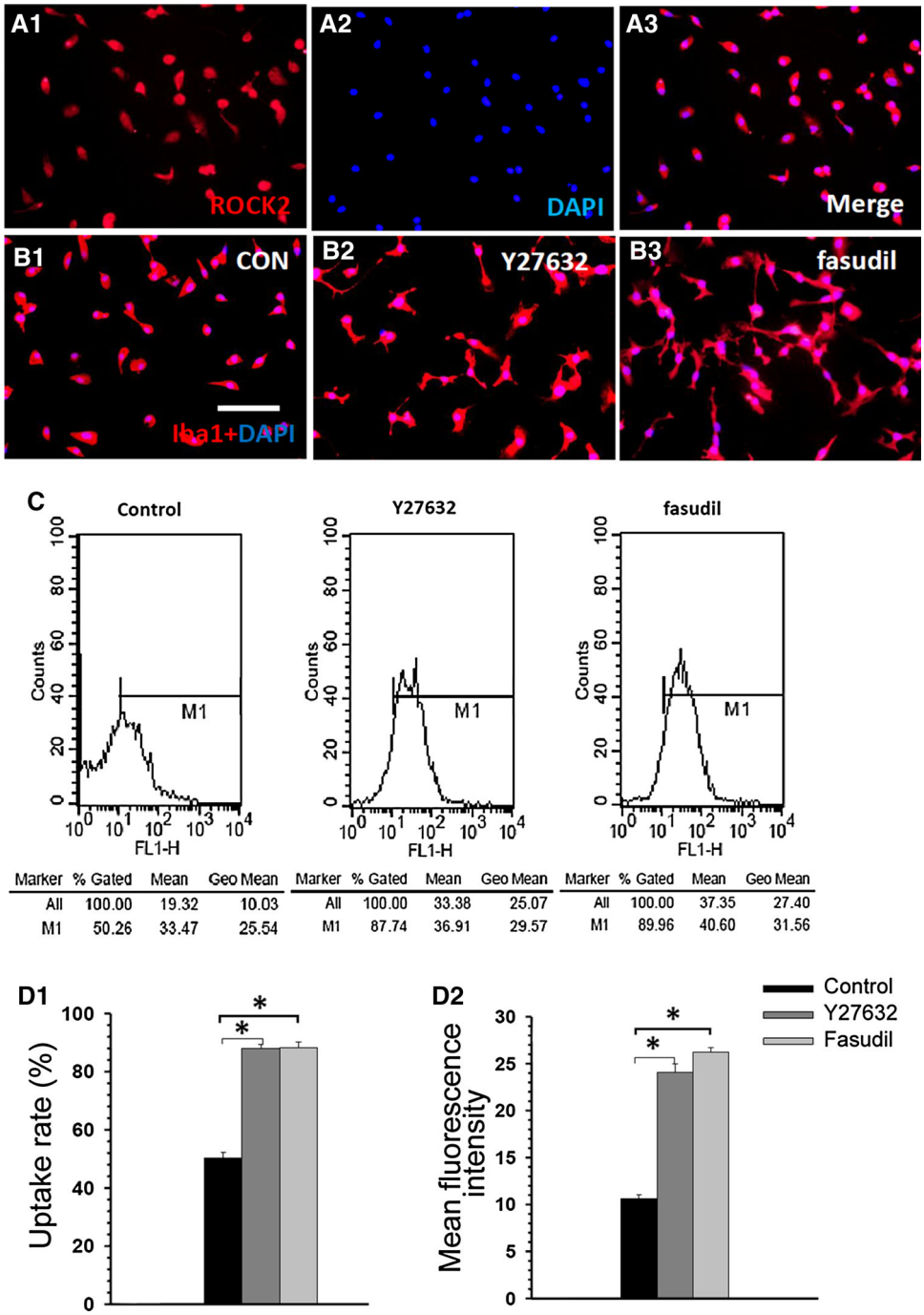

Fig. 3 Y27632 and fasudil changed cell morphology and enhanced uptake activity in primary microglia. (**A**) Expression of ROCK2 identified by staining with anti-ROCK2 (*red*) and DAPI (*blue*). (**B**) Double staining with Iba1 (*red*) and DAPI (*blue*) 1 h after treatment in the control (**B1**), Y27632 (**B2**), and fasudil (**B3**) groups (*scale bar*, 25 μm. (**C**) Representative examples of flow cytometric analysis of control, Y27632-, and fasudil-treated primary microglia at 1 h. (**D**) The data indicated that Y27632 and fasudil stimulated uptake in primary microglia. The percentage of primary microglia that took up FITC-dextran (**D1**) and the mean fluorescence intensity of FITC-dextran (**D2**) in primary microglia increased after Y2762 and fasudil treatment. The results are expressed as the mean ± SEM ($n = 5$, $^*P < 0.01$, Y27632 *vs* control group, fasudil *vs* control group).

uptake activity [24–27]. Western blot analysis showed that treatment with either Y27632 or fasudil (0.5, 1, and 3 h) upregulated the expression of p-ERK ($P < 0.01$ compared with control, Fig. 4), while p-JNK, p-p38, total ERK1/2, total JNK, and total p38 expression were unaffected (Fig. 4A).

Furthermore, BV2 cells were pre-incubated with 10 μmol/L U0126, an inhibitor of ERK1/2 activation [12], for 30 min before Y27632 and fasudil treatment. One hour after Y27632 and fasudil treatment, U0126 markedly reversed the Y27632- and fasudil-induced upregulation of p-ERK expression ($P < 0.01$, Fig. 5A, B) and the uptake enhancement in BV2 cells ($P < 0.01$, Fig. 6A, B). The total ERK1/2 expression remained unchanged (Fig. 5A). Taken together, our results suggested that the ERK signaling pathway plays an important role in Y27632- and fasudil-induced uptake enhancement in BV2 cells.

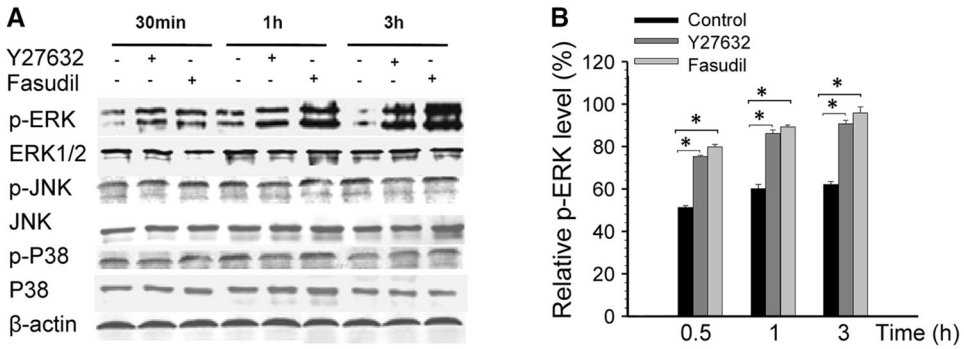

Fig. 4 Effects of Y27632 and fasudil on MAPK proteins in BV2 microglia. (**A**) Representative Western blots showing the changes in p-ERK, total ERK1/2, p-JNK, total JNK, p-p38, and total p38 expression in response to Y27632 and fasudil treatment. (**B**) Statistical analysis of p-ERK protein expression. Levels of p-ERK increased after Y27632 and fasudil treatment at 0.5, 1, and 3 h. The results are expressed as the mean ± SEM ($n = 5$, $^{*}P < 0.01$, Y27632 *vs* control and fasudil *vs* control).

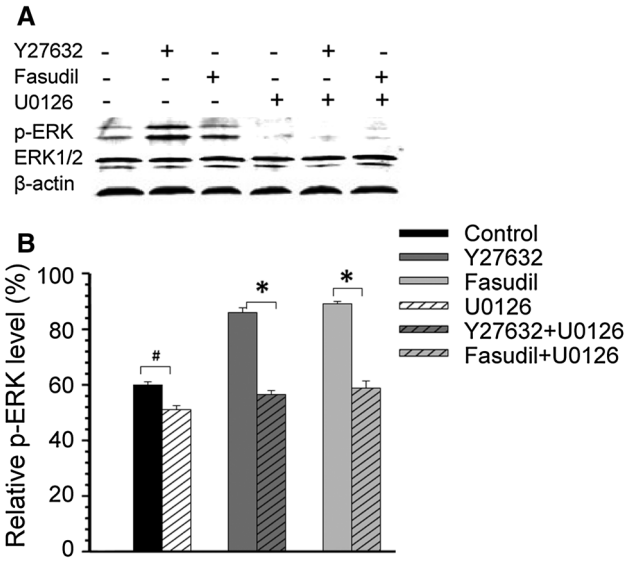

Fig. 5 Effects of Y27632 and fasudil on p-ERK proteins in BV2 microglia. (**A**) Representative Western blots showing the changes in p-ERK expression in response to Y27632, fasudil, U0126, Y27632 plus U0126, and fasudil plus U0126 treatment at 1 h. (**B**) Statistical analysis of p-ERK protein expression. Levels of p-ERK were reduced after U0126 treatment at 1 h, although total ERK1/2 expression remained unchanged. The results are expressed as the mean ± SEM ($n = 5$, $^{*}P < 0.01$, $^{\#}P < 0.05$).

Involvement of the ERK Signaling Pathway in Y27632- and Fasudil-Induced Changes in BV2 Cell Morphology

The morphology of cells treated with U0126 alone (Fig. 6C4) was similar to that of control cells (Fig. 6C1). U0126 added to Y27632- or fasudil-treated cells prevented the Y27632- or fasudil-induced morphological changes (Fig. 6C5, C6). Thus, the ERK signaling pathway is involved in the Y27632- and fasudil-induced morphological changes in BV2 cells, and these changes are associated with uptake enhancement in these cells.

Discussion

Previous studies have demonstrated that ROCK plays important roles in the microglial secretion of inflammatory factors and in the control of microglial morphology and migration [28–32]. Nevertheless, its role in microglial uptake activity and the possible mechanism remain poorly understood. Uptake activity can be divided into pinocytosis and phagocytosis. Pinocytosis is distinguished by morphological examination — macropinocytosis and micropinocytosis. While phagocytosis is generally used to describe the uptake of large solid particles, the term "pinocytosis" refers to fluid intake as well as to the ingestion of materials dissolved or suspended in the fluid phase. Many mammalian cells engulf solid particles such as latex, zymosan (dextran), bacteria, and erythrocytes. Here, we used FITC-dextran (0.1 mg/ml, molecular weight 40,000) which normally occurs in principle by receptor-mediated phagocytosis or by pinocytic pathways in cells, to assess the uptake activity of microglia [33, 34]. We investigated the effect of ROCK inhibition on the uptake activity and cell morphology of microglial cells. Using a specific ROCK inhibitor Y27632 [8], and a nonspecific ROCK inhibitor fasudil [17, 18], we demonstrated that ROCK inhibition increased the uptake activity of microglial cells and was associated with morphological changes.

Accumulating evidence suggests that ROCK inhibition may play an active role in cell uptake activity [4, 35–38]. Changsuk Moon *et al.* have shown that Y27632 inhibition of ROCK enhances the ability of alveolar macrophages to clear apoptotic cells during the intense lung inflammation associated with oxidative stress [39]. The observations of Miri Gitik *et al.* suggest that Rho/ROCK down-regulates

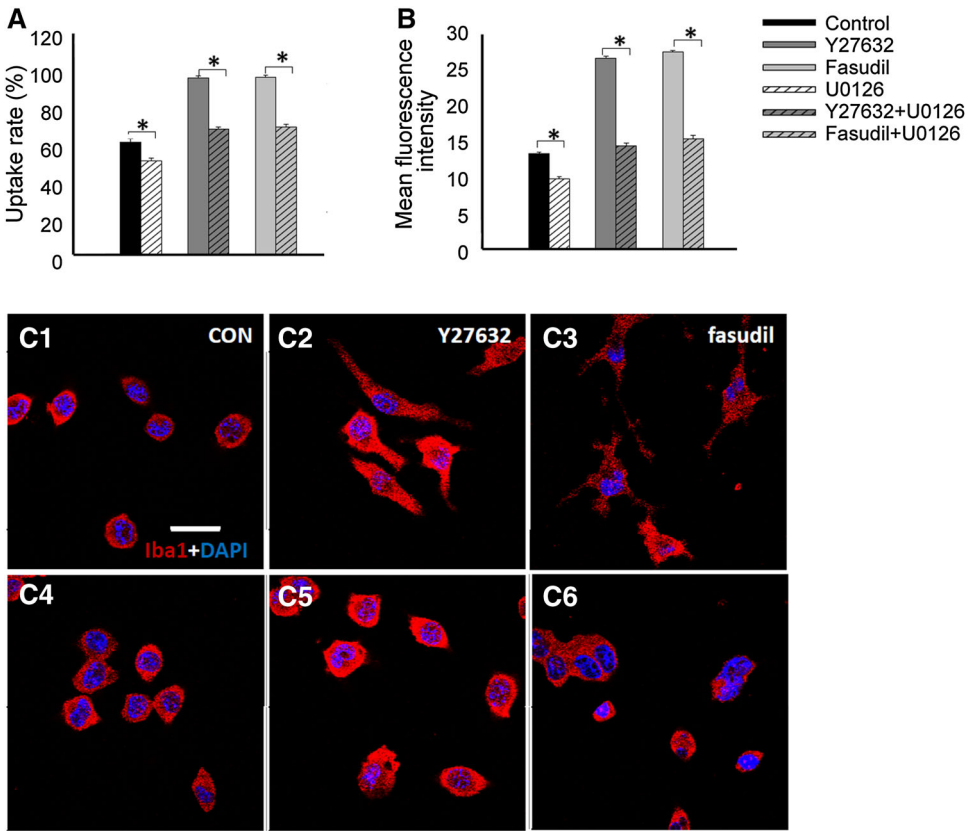

Fig. 6 Involvement of the ERK signaling pathway in the Y27632- and fasudil-induced uptake activity and morphological changes in BV2 microglia. Changes in (**A**) the percentage of BV2 microglia that took up FITC-dextran and (**B**) the mean fluorescence intensity of FITC-dextran in BV2 microglia were dependent on p-ERK protein expression. The results are expressed as the mean ± SEM ($n = 5$, $^*P < 0.01$). (**C**) Morphological changes of BV2 cells double stained with Iba1 (*red*) and DAPI (*blue*) 1 h after treatment in control (**C1**), Y27632 (**C2**), fasudil (**C3**), U0126 (**C4**), Y27632 plus U0126 (**C5**), and fasudil plus U0126 (**C6**) groups (*scale bar*, 10 μm).

the uptake activity of C3bi-opsonized and non-opsonized myelin in microglia [3]. Consistent with these findings, our results showed that ROCK inhibition by Y27632 and fasudil promotes the uptake of FITC-dextran by BV2 microglia and primary microglial cells.

ROCK activation is known to lead to a number of actin–myosin-mediated processes such as cell motility, adhesion, uptake, and morphological changes [40–46]. In the present study, inhibition of ROCK led to striking morphological changes of BV2 cells that were associated with increased uptake activity. Similar to previous studies, our study found that BV2 cells after ROCK blockade had larger cell bodies with many small dendrites and were more irregularly shaped. High Rho and ROCK activities are necessary for the flattening of cells. The expansion or shrinkage of the cell body accompanied by the disappearance or outgrowth of branched processes, respectively, depends on remodeling of the cytoskeleton, a well-known target of Rho GTPases [9]. Morphological changes are also associated with cell adhesion and motility [47, 48]. Previous studies have demonstrated that thrombodulin controls epithelial morphology and promotes cell migration [49]. Hypoxia modulates fibroblastic architecture, adhesion, and migration [50] and the endocytic protein GRAF1 regulates cell-matrix adhesion sites and cell spreading [51]. So to further understand the effect of Rho/ROCK on microglial function, further investigations on microglial migration and adhesion are required.

Several studies have shown that the MAPK signaling pathway is involved in microglial proliferation, inflammatory factor secretion, and uptake activity [24–27]. In the present study, ERK, the most widely studied MAPK cascade, played a crucial role in uptake activity and the morphological changes induced by ROCK inhibition. Inhibition of ROCK by Y27632 and fasudil significantly increased the phosphorylation of ERK1/2 in BV2 cells. Furthermore, U0126, an inhibitor of ERK [12, 52], suppressed the Y27632- and fasudil-induced changes in BV2 cell uptake activity and morphology. Taken together, these results indicate that the ERK signaling pathway mediates the ROCK inhibitor-induced enhancement of uptake activity and is associated with morphological changes by alteration of the actin cytoskeleton. In addition, ROCK inhibition may play a negative role in the uptake activity of some cells under pathological and physiological conditions [36, 53]. Thus, the precise role of ROCK in cell uptake remains controversial and requires further investigation.

In conclusion, ROCK inhibition by Y27632 and fasudil effectively increased the uptake activity of microglial cells and induced changes in cell morphology through the ERK signaling pathway. Understanding the cellular and molecular regulatory mechanisms of ROCK inhibition may help

elucidate the role of ROCK inhibition in CNS development and disease.

Acknowledgments This work was supported by grants from the National Natural Science Foundation of China (81471200 and 81000521), and the National Basic Research Development Program of China (2011CB504403).

References

1. Lawson LJ, Perry VH, Dri P, Gordon S. Heterogeneity in the distribution and morphology of microglia in the normal adult mouse brain. Neuroscience 1990, 39: 151–170.
2. Streit WJ, Conde JR, Fendrick SE, Flanary BE, Mariani CL. Role of microglia in the central nervous system's immune response. Neurol Res 2005, 27: 685–691.
3. Gitik M, Reichert F, Rotshenker S. Cytoskeleton plays a dual role of activation and inhibition in myelin and zymosan phagocytosis by microglia. FASEB J 2010, 24: 2211–2221.
4. Tosello-Trampont AC, Nakada-Tsukui K, Ravichandran KS. Engulfment of apoptotic cells is negatively regulated by Rho-mediated signaling. J Biol Chem 2003, 278: 49911–49919.
5. Swanson JA. Shaping cups into phagosomes and macropinosomes. Nat Rev Mol Cell Biol 2008, 9: 639–649.
6. Pellegrin S, Mellor H. Actin stress fibres. J Cell Sci 2007, 120: 3491–3499.
7. Clark K, Langeslag M, Figdor CG, van Leeuwen FN. Myosin II and mechanotransduction: a balancing act. Trends Cell Biol 2007, 17: 178–186.
8. Ishizaki T, Maekawa M, Fujisawa K, Okawa K, Iwamatsu A, Fujita A, *et al.* The small GTP-binding protein Rho binds to and activates a 160 kDa Ser/Thr protein kinase homologous to myotonic dystrophy kinase. EMBO J 1996, 15: 1885–1893.
9. Matsui T, Amano M, Yamamoto T, Chihara K, Nakafuku M, Ito M, *et al.* Rho-associated kinase, a novel serine/threonine kinase, as a putative target for small GTP binding protein Rho. EMBO J 1996, 15: 2208–2216.
10. Riento K, Ridley AJ. Rocks: multifunctional kinases in cell behaviour. Nat Rev Mol Cell Biol 2003, 4: 446–456.
11. Cox D, Chang P, Zhang Q, Reddy PG, Bokoch GM, Greenberg S. Requirements for both Rac1 and Cdc42 in membrane ruffling and phagocytosis in leukocytes. J Exp Med 1997, 186: 1487–1494.
12. Caron E, Hall A. Identification of two distinct mechanisms of phagocytosis controlled by different Rho GTPases. Science 1998, 282: 1717–1721.
13. Tosello-Trampont AC, Brugnera E, Ravichandran KS. Evidence for a conserved role for CRKII and Rac in engulfment of apoptotic cells. J Biol Chem 2001, 276: 13797–13802.
14. Massol P, Montcourrier P, Guillemot JC, Chavrier P. Fc receptor-mediated phagocytosis requires CDC42 and Rac1. EMBO J 1998, 17: 6219–6229.
15. Gumienny TL, Brugnera E, Tosello-Trampont AC, Kinchen JM, Haney LB, Nishiwaki K, *et al.* CED-12/ELMO, a novel member of the CrkII/Dock180/Rac pathway, is required for phagocytosis and cell migration. Cell 2001, 107: 27–41.
16. Favata MF, Horiuchi KY, Manos EJ, Daulerio AJ, Stradley DA, Feeser WS, *et al.* Identification of a novel inhibitor of mitogen-activated protein kinase kinase. J Biol Chem 1998, 273: 18623–18632.
17. Olson MF. Applications for ROCK kinase inhibition. Curr Opin Cell Biol 2008, 20: 242–248.
18. Miyata K, Shimokawa H, Kandabashi T, Higo T, Morishige K, Eto Y, *et al.* Rho-kinase is involved in macrophage-mediated formation of coronary vascular lesions in pigs in vivo. Arterioscler Thromb Vasc Biol 2000, 20: 2351–2358.
19. John GR, Chen L, Rivieccio MA, Melendez-Vasquez CV, Hartley A, Brosnan CF. Interleukin-1beta induces a reactive astroglial phenotype via deactivation of the Rho GTPase-Rock axis. J Neurosci 2004, 24: 2837–2845.
20. Racchetti G, D'Alessandro R, Meldolesi J. Astrocyte stellation, a process dependent on Rac1 is sustained by the regulated exocytosis of enlargeosomes. Glia 2012, 60: 465–475.
21. Ding J, Li QY, Wang X, Sun CH, Lu CZ, Xiao BG. Fasudil protects hippocampal neurons against hypoxia-reoxygenation injury by suppressing microglial inflammatory responses in mice. J Neurochem 2010, 114: 1619–1629.
22. Kato M, Neil TK, Fearnley DB, McLellan AD, Vuckovic S, Hart DN. Expression of multilectin receptors and comparative FITC-dextran uptake by human dendritic cells. Int Immunol 2000, 12: 1511–1519.
23. Hu X, Zhang W, Wang L, Wan N, Wang B, Li W, *et al.* The detailed analysis of the changes of murine dendritic cells (DCs) induced by thymic peptide: pidotimod(PTD). Hum Vaccin Immunother 2012, 8: 1250–1258.
24. Miao J, Ding M, Zhang A, Xiao Z, Qi W, Luo N, *et al.* Pleiotrophin promotes microglia proliferation and secretion of neurotrophic factors by activating extracellular signal-regulated kinase 1/2 pathway. Neurosci Res 2012, 74: 269–276.
25. Calvo M, Zhu N, Grist J, Ma Z, Loeb JA, Bennett DL. Following nerve injury neuregulin-1 drives microglial proliferation and neuropathic pain via the MEK/ERK pathway. Glia 2011, 59: 554–568.
26. Ellert-Miklaszewska A, Dabrowski M, Lipko M, Sliwa M, Maleszewska M, Kaminska B. Molecular definition of the pro-tumorigenic phenotype of glioma-activated microglia. Glia 2013, 61: 1178–1190.
27. Martin R, Cordova C, Nieto ML. Secreted phospholipase A2-IIA-induced a phenotype of activated microglia in BV-2 cells requires epidermal growth factor receptor transactivation and proHB-EGF shedding. J Neuroinflammation 2012, 9: 154.
28. Hoffmann A, Hofmann F, Just I, Lehnardt S, Hanisch UK, Bruck W, *et al.* Inhibition of Rho-dependent pathways by Clostridium botulinum C3 protein induces a proinflammatory profile in microglia. Glia 2008, 56: 1162–1175.
29. Yan J, Zhou X, Guo JJ, Mao L, Wang YJ, Sun J, *et al.* Nogo-66 inhibits adhesion and migration of microglia via GTPase Rho pathway in vitro. J Neurochem 2012, 120: 721–731.
30. Schwab JM, Conrad S, Elbert T, Trautmann K, Meyermann R, Schluesener HJ. Lesional RhoA + cell numbers are suppressed by anti-inflammatory, cyclooxygenase-inhibiting treatment following subacute spinal cord injury. Glia 2004, 47: 377–386.
31. Takenouchi T, Iwamaru Y, Sugama S, Sato M, Hashimoto M, Kitani H. Lysophospholipids and ATP mutually suppress maturation and release of IL-1 beta in mouse microglial cells using a Rho-dependent pathway. J Immunol 2008, 180: 7827–7839.
32. Bernhart E, Kollroser M, Rechberger G, Reicher H, Heinemann A, Schratl P, *et al.* Lysophosphatidic acid receptor activation affects the C13NJ microglia cell line proteome leading to alterations in glycolysis, motility, and cytoskeletal architecture. Proteomics 2010, 10: 141–158.
33. Silverstein SC, Steinman RM, Cohn ZA. Endocytosis. Annu Rev Biochem 1977, 46: 669-722.
34. Michl J. Receptor mediated endocytosis. Am J Clin Nutr 1980, 33: 2462–2471.
35. Anand RJ, Dai S, Gribar SC, Richardson W, Kohler JW, Hoffman RA, *et al.* A role for connexin43 in macrophage phagocytosis and host survival after bacterial peritoneal infection. J Immunol 2008, 181: 8534–8543.

36. Orlando KA, Pittman RN. Rho kinase regulates phagocytosis, surface expression of GlcNAc, and Golgi fragmentation of apoptotic PC12 cells. Exp Cell Res 2006, 312: 3298–3311.
37. Boe DM, Richens TR, Horstmann SA, Burnham EL, Janssen WJ, Henson PM, *et al.* Acute and chronic alcohol exposure impair the phagocytosis of apoptotic cells and enhance the pulmonary inflammatory response. Alcohol Clin Exp Res 2010, 34: 1723–1732.
38. Shi J, Wei L. Rho kinase in the regulation of cell death and survival. Arch Immunol Ther Exp (Warsz) 2007, 55: 61–75.
39. Moon C, Lee YJ, Park HJ, Chong YH, Kang JL. N-acetylcysteine inhibits RhoA and promotes apoptotic cell clearance during intense lung inflammation. Am J Respir Crit Care Med 2010, 181: 374–387.
40. Zhou Q, Gensch C, Liao JK. Rho-associated coiled-coil-forming kinases (ROCKs): potential targets for the treatment of atherosclerosis and vascular disease. Trends Pharmacol Sci 2011, 32: 167–173.
41. Khyrul WA, LaLonde DP, Brown MC, Levinson H, Turner CE. The integrin-linked kinase regulates cell morphology and motility in a rho-associated kinase-dependent manner. J Biol Chem 2004, 279: 54131–54139.
42. Leemhuis J, Boutillier S, Schmidt G, Meyer DK. The protein kinase A inhibitor H89 acts on cell morphology by inhibiting Rho kinase. J Pharmacol Exp Ther 2002, 300: 1000–1007.
43. Honjo M, Tanihara H, Inatani M, Kido N, Sawamura T, Yue BY, *et al.* Effects of rho-associated protein kinase inhibitor Y-27632 on intraocular pressure and outflow facility. Invest Ophthalmol Vis Sci 2001, 42: 137–144.
44. Mammoto A, Huang S, Moore K, Oh P, Ingber DE. Role of RhoA, mDia, and ROCK in cell shape-dependent control of the Skp2-p27kip1 pathway and the G1/S transition. J Biol Chem 2004, 279: 26323–26330.
45. Rousseau M, Gaugler MH, Rodallec A, Bonnaud S, Paris F, Corre I. RhoA GTPase regulates radiation-induced alterations in endothelial cell adhesion and migration. Biochem Biophys Res Commun 2011, 414: 750–755.
46. Kitzing TM, Sahadevan AS, Brandt DT, Knieling H, Hannemann S, Fackler OT, *et al.* Positive feedback between Dia1, LARG, and RhoA regulates cell morphology and invasion. Genes Dev 2007, 21: 1478–1483.
47. Lino N, Fiore L, Rapacioli M, Teruel L, Flores V, Scicolone G, *et al.* uPA-uPAR molecular complex is involved in cell signaling during neuronal migration and neuritogenesis. Dev Dyn 2014, 243: 676–689.
48. Wang SC, Lin XL, Li J, Zhang TT, Wang HY, Shi JW, *et al.* MicroRNA-122 triggers mesenchymal-epithelial transition and suppresses hepatocellular carcinoma cell motility and invasion by targeting RhoA. PLoS One 2014, 9: e101330.
49. Hsu YY, Shi GY, Kuo CH, Liu SL, Wu CM, Ma CY, *et al.* Thrombomodulin is an ezrin-interacting protein that controls epithelial morphology and promotes collective cell migration. FASEB J 2012, 26: 3440–3452.
50. Vogler M, Vogel S, Krull S, Farhat K, Leisering P, Lutz S, *et al.* Hypoxia modulates fibroblastic architecture, adhesion and migration: a role for HIF-1alpha in cofilin regulation and cytoplasmic actin distribution. PLoS One 2013, 8: e69128.
51. Doherty GJ, Ahlund MK, Howes MT, Moren B, Parton RG, McMahon HT, *et al.* The endocytic protein GRAF1 is directed to cell-matrix adhesion sites and regulates cell spreading. Mol Biol Cell 2011, 22: 4380–4389.
52. Villanueva J, Yung Y, Walker JL, Assoian RK. ERK activity and G1 phase progression: identifying dispensable versus essential activities and primary versus secondary targets. Mol Biol Cell 2007, 18: 1457–1463.
53. Kim JS, Kim JG, Jeon CY, Won HY, Moon MY, Seo JY, *et al.* Downstream components of RhoA required for signal pathway of superoxide formation during phagocytosis of serum opsonized zymosans in macrophages. Exp Mol Med 2005, 37: 575–587.